Self-consistent model for the nonequilibrium cathode region

P. Bayle* and A. Perrin
Ecole Nationale Supérieure de Physique de Strasbourg, 7, Rue de l'Université, 67000 Strasbourg, France
(Received 22 January 1992; revised manuscript received 24 July 1992)

We present a theoretical study and a numerical simulation of the formation and development of the cathode region (cathode-fall and negative-glow ones) in CO_2 and N_2 discharges from the inception of the discharge to its stationary state. The model is a self-consistent one: the distribution of the electric field is found from the charge carriers and the hydrodynamic moment equations (density, velocity, energy) are solved by a sophisticated flux-corrected transport method. The ionization and excitation source terms are calculated using an electron-energy distribution function which takes into account the electron-density gradient and the local electric field. The results show that this choice is more realistic in representing the spatiotemporal evolution of the cathode region. Our theoretical results are compared with the experimental ones obtained by other authors and a good agreement is observed concerning the current intensity and the spatial distribution of light in the cathode region in N_2.

PACS number(s): 52.25.Fi, 52.65.+z, 52.80.−s

I. INTRODUCTION

The conditions existing in the cathode region greatly influence the electron behavior that no longer depends on the value of the local electric field. The electron gas evolves in nonhydrodynamic conditions, and the energy reached by an electron in space $\vec{r}$ and time t is not instantaneously lost by collisions. Such a behavior, which greatly differs from the classic hydrodynamic situation, has been theoretically studied by different means.

Monte Carlo–like methods "dealing with particles" have been greatly developed. Boeuf and Marode [1] described a Monte Carlo method for studying the steady-state behavior of charged species in helium under the influence of a nonuniform electric field. Moratz, Pitchford, and Bardsley [2] studied the transport of electrons through a background of nitrogen gas under the influence of spatially varying electric field through a Monte Carlo simulation. Nonhydrodynamic effects, i.e., a nonlocal dependency of the electron transport and rate coefficients on the ratio of the field strength to the neutral density E/N, are observed. These authors assumed *a priori* that the field distribution is linear with two regions of uniform field which separate the varying field from boundary effects. This field partition fixes the effect of the nonhydrodynamic situation on the electronic parameters of the discharge in the varying electric field region. They observed that the spatial evolution of the swarm in the decreasing field is different from that of the increasing field.

Beside Monte Carlo simulation techniques, the theoretical study of cathode fall has been carried out, solving the successive moments of the Boltzmann equation. Sommerer, Lawler, and Hitchon [3] proposed a model for the cathode-fall region of a dc glow discharge. The zeroth and second moments of the Boltzmann equation are solved for the electrons with a self-consistent electric field. A single model with only two parameters (number density and beam velocity) is assumed for the electron-distribution function. Their paper presented an interesting necessary extremum condition that specifies a correct electric-field distribution in cathode fall and the lower field in the negative glow was imposed as 10 V/cm. The results are in good qualitative agreement with Doughty, Den Hartog, and Lawler [4]. Phelps, Jelenkovic, and Pitchford [5] investigated a similar single-beam model using number-density and beam-energy equations. Sommerer, Hitchon, and Lawler [6] modeled the electron behavior in the cathode fall of a helium dc glow discharge with a self-consistent electric field using a "convective scheme." The field predicted by the self-consistent calculations is in excellent agreement with optogalvanic experiments.

For the study of the cathode fall and the negative glow in a transitory discharge in CO_2, Bayle, Vacquie, and Bayle [7] proposed a self-consistent model based on the continuity equations of the density of charge carriers (electrons, positive and negative ions) of the moment equation and the electron-energy equation, associated to the equation of Poisson.

The deviation from the hydrodynamic conditions is mainly a function of the gradients appearing in the discharge, that is to say, field gradients as shown by Monte Carlo simulation by Moratz, Pitchford, and Bardsley [2] with increasing or decreasing fixed gradients of field or by field and electron-density gradients as shown in self-consistent models used to study the ionization waves or the cathode-fall inception by Bayle and coworkers [7–9].

For this reason, we present in this paper an extension of the model proposed by Bayle, Vacquie, and Bayle [7] by taking into account the effects of the field and density gradients on the electron-energy-distribution function. This model is tested in two experimental situations: First, the study of the inception of the cathode zone in a glow discharge in CO_2 up to the stationary state. Second, the simulation of the experiment of Bastien, Wu, and Marode [10] in which the inception of the cathode zone in N_2 is followed to the stationary state. A good agree-

ment is obtained between the experimental measurements of the light emission and those obtained by the numerical simulation.

II. MODEL

A. Physical hypothesis

The discharge model is a monodimensional one in which the main effects of electron multiplication, drift, and diffusion are functions only of the position between the electrodes. The losses by radial diffusion are negligible. The space-charge electric field is obtained by solving the monodimensional equation of Poisson. With the hypothesis of a slightly ionized gas, the neutral gas density remains constant. The neutral gas plays the role of an infinite sink of energy and remains at the same temperature.

The (positive and negative) ions are in hydrodynamic equilibrium with the electric field, hence the ionic movement is simply linked to the local electric field by the mobility relation. This hypothesis, used in our preceding papers, has been corroborated by Lawler [11]. He stated that for the ions in helium, the parametrization of the velocity by the mobility is correct for high electric field zones and that in rapidly varying electric field, the ions need some (1 to 6) mean free paths to reach the velocity stated by the mobility versus the electric field. As we work on heavier ions, and with the fine spatial mesh used for solving the equations, the ions are supposed to be in equilibrium with the electric field.

We choose to simulate the discharge by means of a mixed microscopic macroscopic formalism, extrapolated from that developed in the previous papers by Bayle and co-workers [7–9]. It is based on the equations of the first moments of Boltzmann equation, continuity equations for electronic and ionic densities, the momentum equation, and the electron-energy equation, but the collisional operators for ionization, excitation, momentum transfer, and energy transfer are a function of the local electron energy and some of them are explicitly written from the microscopic distribution function. This formalism preserves all the benefits of the hydrodynamic formalism particularly to find self-consistent solutions which are more difficult to obtain through particles or microscopic methods. It is clear, however, that the quality of results obtained is highly functional of the coupling between the microscopic scheme and the macroscopic scheme and of the way for the nonhydrodynamic condition to be taken into account both in the microscopic and macroscopic points of view. In hydrodynamic conditions, the energy reached by an electron along a mean free path can be considered as instantaneously lost by collisions. There is a direct equilibrium between energy gain and loss and the energy of the electrons is directly linked to the electric field, the collisional frequencies being completely defined by the knowledge of the local electric field. In the nonhydrodynamic condition, the energy gained by an electron is not instantaneously lost by collisions. All is going on as if a relaxation time or a relaxation length exists to reach equilibrium between energy gain and loss. Two parameters are significant to characterize the divergence from the hydrodynamic situation: the ratio of the electric field on neutral molecules density E/N and the gradients (mainly the electron density gradient). This implies that, in nonhydrodynamic conditions, the use of classical macroscopic coefficients, measured at very low current density and in spatially invariant electric fields, is called into question and these coefficients have to be estimated. The collision frequencies appearing in the three moment equations have to be parametrized by average electron energy rather than explicitly by E/N. However, it is necessary to separate the collisional processes induced by all the electrons (as momentum and energy exchanges) from those due to the part of electrons whose energy is greater than a given threshold (as ionization and excitation processes). It is obvious that the nonequilibrium effects affect more the macroscopic coefficients that depend on the tail of the distribution function and less those depending on the bulk of this distribution function. So, the collisional frequencies of momentum transfer and energy transfer are less modified by the nonequilibrium between electrons and electric field than the collisional excitation and ionization frequencies. This implies that, if the expressions of the ionization and excitation source terms need specification of the distribution function, i.e., a microscopic representation of the discharge, the expressions of collisional source terms in momentum and energy equations which depends mainly on the bulk of the distribution function, can simply be described by a macroscopic approach.

B. Nonequilibrium distribution function

The cathodic zone is a zone with strong gradients of electric field and electronic densities. These gradients greatly modify the electron distribution function. This dependence of the electron-energy distribution function (EEDF) with the gradient of electron densities has largely been confirmed by experimental work for pulsed and steady streams by Wedding, Blevin, and Fletcher [12] and Wedding and Kelly [13]. Using photon-flux techniques, they studied the spatial variation of the relative excitation rates for two electronic states of molecular nitrogen. The ratio of these rates shows a spatial dependence which is explained in terms of an electron concentration gradient expansion of the energy distribution function. Thomas [14] and Kumar, Skullerud, and Robson [15] have shown that in Townsend discharges, the EEDF is a function of the ratio of electric field strength on the concentration of the neutral gas molecule density and also a function of the local gradient of electron concentration. Kumar, Skullerud, and Robson [15] have formulated the distribution as an expansion of a series of powers of relative gradient of electron densities. The expression of the EEDF as an expansion of a series is not easy to use in a numerical scheme for the calculation of source terms, for example. Lucas [16] gave an analytical formulation of the EEDF (including the effect of the relative gradient of electron densities), which is easy to use for the calculation of ionization frequencies. This relation is obtained from an approached solution of Boltzmann's equation, with the hypothesis of a stationary discharge without space

charge, i.e., at constant electric field and temperature. In our numerical simulation, we use this relation even if its use for the study of the spatiotemporal evolution of the cathodic zone seems inadequate. As the direct experiment determination of the EEDF is generally impossible, the validity of an EEDF may be stated by its macroscopic results, i.e., by the variations of the diffusion coefficient and of the diffusion velocity that indirectly show the spatial change in the EEDF. More indirect evidence of the variation of EEDF are the values of the ionization and excitation frequencies which are greater when the electron density gradient is negative (or smaller when positive) than the values calculated as a function of E/N alone. Wedding stated in his work that the EEDF is a function of the gradient of electronic density as well in pulsed streams as in steady streams. Then, we use the Lucas formulation, and the validation check point of this method is made by the simulation of the cathode-zone evolution and the correlation with the experimental results. Lucas proposed a distribution function that specifies the role of the gradient by

$$f_L(\varepsilon)=f_0(\varepsilon)\exp\left[-\int_0^{\varepsilon}\frac{1}{eE}\frac{1}{n_e}\frac{\partial n_e}{\partial x}d\varepsilon\right], \tag{1}$$

where $f_0(\varepsilon)$ is a stationary solution without gradient.

As the bulk of the distribution function is nearly Maxwellian and as the perturbations mainly affect the tail, we chose to express $f_0(\varepsilon)$ as a Maxwellian function at the temperature T_e defined by the energy equation. The distribution function f_L is normalized by

$$\int_0^{\infty}\sqrt{\varepsilon}f_L(\varepsilon)d\varepsilon=1, \tag{2}$$

then, the EEDF of Lucas is

$$f_L(\varepsilon)=\frac{2}{\sqrt{\pi}}\varepsilon^{1/2}\left[\frac{kT}{1+\frac{1}{n}\frac{\partial n}{\partial x}\frac{kT}{eE}}\right]^{-3/2}\exp\left[-\varepsilon\Big/\left[\frac{kT}{1+\frac{1}{n}\frac{\partial n}{\partial x}\frac{kT}{eE}}\right]\right]. \tag{3}$$

This EEDF looks like a Maxwellian distribution function in which the temperature kT has been replaced by $kT/[1+(kT\nabla \ln n)/eE]$. In other words, Lucas's EEDF is equivalent to a Maxwellian EEDF whose mean energy is lower than kT in the cathode-fall region where the gradient is positive. In these conditions, the source terms (ionization, attachment) playing a role in the continuity equation for electron and ion densities and the excitation term used in the secondary effects at the cathode are formulated by

$$S_j(T_e,n_e,N)=Nn_e\int_0^{\infty}\sigma_j(\varepsilon)w(\varepsilon)f_L(\varepsilon)d\varepsilon, \tag{4}$$

where $\sigma_j(\varepsilon)$ is the cross section for the collisional process involved (ionization, attachment, excitation).

From this point of view, the mean energy used for the calculation of the ionization and excitation source terms appears as lower than the mean energy calculated by the energy equation. This is linked to a "corrected" effect of the density gradients. The two values of the mean energy are the same when

$$\frac{kT}{eE}\nabla \ln n \ll 1. \tag{5}$$

In this case, Lucas's EEDF is equivalent to a Maxwellian EEDF.

In the analysis of the results of our simulation, it will appear that the use of this EEDF gives very interesting results in good agreement with the experimental results. This is probably linked to the fact that the cathode zone in molecular gases is different from that of atomic gases, mainly because of the great numbers of excited stated (rotational, vibrational, and electronic states). This implies that the specific energy losses appearing in atomic gases in a well-determined energy range cannot appear in molecular gases, such as those studied in this paper. In molecular gases, the energy losses are more distributed due to the broadness of the elastic and inelastic cross sections. A distribution function with a Maxwellian shape and taking into account the gradient effects may be a good representation for the electrons. When the electric field and the density gradient are too weak, the term $(1/eE)(1/n_e)(\partial n_e/\partial x)$ may have an artificial weight in the distribution function stated by Lucas, without connection with the nonhydrodynamic situation. For these conditions of weak local electric field, we assumed that the elastic collisions play a more major role than the inelastic collisions and thus the distribution becomes Maxwellian. In this case also, the temperature is that deduced from the energy equation and this involves nonequilibrium in the expression of the distribution function.

C. General formalism

The formalism, used in this work, comments on the transport equations for densities (electrons, positive and negative ions) and momentum and energy equations for electrons only. In these equations, the operators for momentum and energy transfer are stated macroscopically as previously done by Bayle and co-workers [7–9] whereas the ionization and excitation source terms are directly calculated by means of the distribution function and of the corresponding cross section.

The effects of the density gradients are taken into account, in a macroscopic point of view, in the moment equation by $\partial(n_eT_e)/\partial x$ and in the energy equation by $\partial(n_eT_eu_e)/\partial x$ and in a microscopic point of view by the modification of the distribution function. Some examples of the role of these gradients on nonequilibrium are shown in [8].

1. Continuity equations

For electrons,

$$\frac{\partial n_e}{\partial t}+\frac{\partial(n_e u_e)}{\partial x}=S_{\text{ion}}-S_{\text{att}} \ . \tag{6}$$

For negative ions (for CO_2 only),

$$\frac{\partial n^-}{\partial t}+\frac{\partial(n^- u^-)}{\partial x}=S_{\text{att}} \ . \tag{7}$$

For positive ions,

$$\frac{\partial n_+}{\partial t}-\frac{\partial(n_+ u_+)}{\partial x}=S_{\text{ion}} \ . \tag{8}$$

n_e, n^-, n_+ are, respectively, the electron, negative-ion, and positive-ion densities. u_e, u^-, u_+ are the corresponding velocities.

S_{ion}, S_{att} are the collisional source terms for ionization and attachment (for CO_2 only), defined by Eq. (4) from the distribution function defined versus the electronic temperature T_e as deduced from the energy equation, from the relative local gradient of electron density, and from electric field.

2. Momentum equation

The positive and negative ions are assumed to be in equilibrium with the electric field. Thus, their velocities are settled versus the electric field from the drift experimental results.

As the cathode zone is greatly nonhydrodynamic, the momentum transfer equation is used to calculate the electron velocity, as explained in [7]. This equation takes Eq. (6) into account:

$$\frac{\partial u_e}{\partial t}+u_e\frac{\partial u_e}{\partial x}=\frac{e}{m_e}E-\frac{e}{m_e n_e}\frac{\partial(n_e T_e)}{\partial x}-u_e\frac{S_{\text{ion}}-S_{\text{att}}}{n_e}-\frac{(\nabla^e+\nabla^i)(m_e w_e)}{m_e n_e} \ . \tag{9}$$

$(\nabla^e+\nabla^i)(m_e w_e)$ is the operator for momentum transfer in elastic and inelastic collisions.

As explained in [7], this operator has the same dependence on temperature as in the hydrodynamic state, but the temperature involved is that deduced from the energy equation. In the hydrodynamic situation, i.e., with equilibrium, the operator for momentum transfer is

$$(\nabla^e+\nabla^i)(m_e w_e)=n_e m_e u_e \nu_e(E/N) \ , \tag{10}$$

$\nu_e(E/N)$ is the collision frequency, a function of E/N, and is linked to mobility by

$$\nu_e(E/N)=\frac{e}{m_e}\frac{1}{\mu_e(E/N)} \tag{11}$$

or

$$\nu_e(T_{es})=\frac{e}{m_e}\frac{1}{\mu_e(\Psi(T_{es})/N)} \ .$$

T_{es} is the equilibrium temperature (or static temperature).

In the nonhydrodynamic situation, the same relation is used, but the collision frequency is a function of the true temperature T_e, i.e., the temperature deduced from the energy equation:

$$\nu_e(T_e)=\frac{e}{m_e}\frac{1}{\mu_e\left[\dfrac{\Psi(T_e)}{N}\right]} \tag{12}$$

and thus the operator for momentum transfer is

$$(\nabla^e+\nabla^i)(m_e w_e)=n_e m_e u_e \nu(T_e) \ . \tag{13}$$

The equation of momentum transfer becomes

$$\frac{\partial u_e}{\partial t}+u_e\frac{\partial u_e}{\partial x}=\frac{e}{m}\left[E-\frac{1}{n_e}\frac{(\partial n_e T_e u_e)}{\partial x}\right]-u_e\frac{S_{\text{ion}}-S_{\text{att}}}{n_e}-u_e\nu_e(\Psi(T_e)) \ . \tag{14}$$

3. Energy equation

This equation expresses, from a macroscopic point of view, the nonequilibrium, i.e., the nonhydrodynamic state of the discharge. The electron-energy equation deduced from the Boltzmann equation is

$$\frac{3}{2}\left[\frac{\partial T_e}{\partial t}+u_e\frac{\partial T_e}{\partial x}\right]=u_e E-\frac{1}{n_e}\frac{\partial n_e T_e u_e}{\partial x}-\tfrac{3}{2}T_e(S_{\text{ion}}-S_{\text{att}})-\frac{1}{n_e}(\nabla^e+\nabla^i)(\tfrac{1}{2}m_e w_e^2) \ ,$$

where $(\nabla^e+\nabla^i)(\frac{1}{2}mw_e^2)$ is the energy-transfer operator.

In the hydrodynamic situation, this operator states that the balance between energy gain and energy loss is achieved. Thus,

$$n_e E_s v_d=\tfrac{3}{2}T_{es}(S_{\text{ion}}-S_{\text{att}})+(\nabla^e+\nabla^i)(\tfrac{1}{2}m_e w_e^2) \ . \tag{16}$$

T_{es} is the equilibrium static temperature, v_d is the drift velocity, and E_s is the uniform and static electric field.

In the hydrodynamic situation, there is a direct correspondence between electric field and temperature. $T_{es}=f(E_s)$ or $E_s=\Psi(T_{es})$ and the operator $(\nabla^e+\nabla^i)(\frac{1}{2}m_e w_e^2)$ can be expressed as a function of this static temperature:

$$(\nabla^e+\nabla^i)(\tfrac{1}{2}m_e w_e^2)=n_e\Psi(T_{es})v_d(\Psi(T_{es}))-\tfrac{3}{2}T_{es}[S_{\text{ion}}(T_{es})-S_{\text{att}}(T_{es})] \ . \tag{17}$$

If the same formal relation (towards energy deduced from the energy equation) is assumed in the nonequilibrium situation (or nonhydrodynamic situation) we obtain

$$(\nabla^e+\nabla^i)(\tfrac{1}{2}m_e w_e^2)=n_e\Psi(T_e)v_d(\Psi(T_e))-\tfrac{3}{2}T_e[S_{\text{ion}}(T_e)-S_{\text{att}}(T_e)] \tag{18}$$

and the energy equation becomes

$$\frac{3}{2}\left[\frac{\partial T_e}{\partial t}+u_e\frac{\partial T_e}{\partial x}\right]=u_eE-\frac{1}{n_e}\frac{\partial(n_eT_eu_e)}{\partial x}-\Psi(T_e)v_d(\Psi(T_e))\ . \tag{19}$$

4. *Electric field*

The electric field is calculated from Poisson's equation,

$$\frac{\partial E}{\partial x}=\frac{e}{\varepsilon_0}(n_+-n_e-n^-)\ , \tag{20}$$

and the field is assigned to verify the relation

$$V_G=\int_0^d E(x)dx\ . \tag{21}$$

V_G is the voltage applied to the gap and is defined in the problem.

This condition is always respected in our simulation even if there is local weak field inversion, on the side of the negative glow, in CO_2 as well as in N_2.

The improvement of numeric schemes, compared to previous work [7], makes it possible to obtain a field completely self-consistent with the charge carriers even if field inversion zones appear which are difficult to analyze. Bayle, Vacquie, and Bayle [7] set the electric field value in negative glow to 10 V/cm to avoid field inversion and the same process has been set up again (with the same field value) by Sommerer, Lawler, and Hitchon [3].

5. *Boundary conditions*

At the cathode. The cathode is considered as an electron source through ionic and photonic impact,

$$J_e(0,t)=\gamma_+J_+(0,t)+\gamma_{ph}\int_0^d S_{exc}(x,t)dx\ , \tag{22}$$

with $\gamma_+=5\times10^{-2}$ and $\gamma_{ph}=10^{-4}$ (the average values are equal for CO_2 and N_2).

The excitation source term $S_{exc}(x,t)$ is calculated from Eq. (4) by means of cross sections. For CO_2, we used the formula already given in [7] with the cross sections obtained by Kucukarpaci and Lucas [17].

For N_2, we chose the cross sections given by Hartmann [18] and approximated by the following relation.

First negative system.

$$[\sigma_{1S^-}\ (10^{-18}\ \text{cm}^2)]=\sum_{i=1}^{3}K_i(\varepsilon_i-w_i)[\Delta(\varepsilon-w_{ia})-\Delta(\varepsilon-w_{ib})]+K_4\Delta(\varepsilon-w_4)\ ; \tag{23}$$

ε is the electron energy in electron volts and Δ is the Heaviside step function with

$K_1=0.4507$	$K_2=0.14667$	$K_3=0.03667$	$K_4=15$
$w_1=18.7$	$w_2=-29.318$	$w_3=309.69$	$w_4=63.9$
$w_{1a}=18.7$	$w_{2a}=41.9$	$w_{3a}=63.9$	
$w_{1b}=41.9$	$w_{2b}=63.9$	$w_{2b}=100$	

Second positive system.

$$[\sigma_{2S^+}\ (10^{-18}\ \text{cm}^2)]=\sum_{i=1}^{4}K_i(\varepsilon_i-w_i)[\Delta(\varepsilon-w_{ia})-\Delta(\varepsilon-w_{ib})]\ , \tag{24}$$

with

$K_1=3.9$	$K_2=1.36$	$K_3=0.14286$	$K_4=0.0135$
$w_1=11$	$w_2=-29.318$	$w_3=309.69$	$w_4=180.76$
$w_{1a}=11$	$w_{2a}=14$	$w_{3a}=19$	$w_{4a}=19$
$w_{1b}=14$	$w_{2b}=19$	$w_{2b}=40$	$w_{4b}=w_4$

The total source term is obtained by combining the second positive and first negative source terms

$$S_{exc}=3.5S_{2S^+}+1.5S_{1S^-}\ . \tag{25}$$

As the cross sections only take into account the 0-0 transition, we balance the source terms to introduce the other transitions.

At the anode. The positive-ion density is given by

$$n_+(d,t+\Delta t)=n_+(d,t)+S_{ion}(T_e,n_e,N,t+\Delta t/2)\Delta t\ . \tag{26}$$

Remark. The relation $T_e(x,t)=\Psi(E(x,t)/N)$ and the drift ionic and electronic velocities are the same as those used in [7] for CO_2 and [9] for N_2.

Compared to the results established in [7], the extraction conditions for secondary electrons have been slightly modified. The energy of the emitted electrons is assumed to be equal to 10 eV, according to a series of preceding tests [9].

6. *Initial conditions*

The aim of this section is to settle the way the cathode region is established from a transitory state to obtain the stationary state of a glow discharge.

For the two analyzed gases, an initial decreasing electric field is assumed, defined as follows:

(a) In CO_2. The initial conditions that correspond to some tens of nanoseconds after the application of the voltage impulse are those of experimental work of Cobine [19], Ivanchenko and Shepelenko [20], and Francis [21].

The initial electric field is

$$E(x)=(E_A-E_C)\frac{x}{d}+E_C\ . \tag{27}$$

$E_C=12\,400$ V/cm is the electric field at the cathode,

$E_A = 500$ V/cm is the electric field at the anode, $d = 6.4 \times 10^{-2}$ cm is the cathode-region length, P is the pressure $P = 20$ Torr, $n_e(x)$ is the electron density, with

$$n_e(x) = n_e(0)\exp(\bar{\alpha}x) , \tag{28}$$

with $n_e(0) = 10^{-12}$ C cm^{-3}, $\bar{\alpha} = 71.956$ cm^{-1}. The positive-ion density is

$$n_+(x) \sim \varepsilon_0 \frac{\partial E}{\partial x} = 1.65 \times 10^{-8} \text{ C cm}^{-3} , \tag{29}$$

and negative-ion density

$$n_-(x) \sim 0 . \tag{30}$$

(b) In N_2. The electric field is defined by the same relation with $E_C = 563.3$ V/cm as the electric field at the cathode, $E_A = 5.7$ V/cm as the electric field at the anode, $d = 2$ cm is the gap length, and $P = 1$ Torr.

Remark. Bastien, Wu, and Marode [10] explain that in their experiment the voltage presents a low overshoot after which the voltage reaches the value pointed in their paper. Simulating their experiment, we found that this voltage corresponds to a stabilization voltage, i.e., the voltage corresponding to a stationary state of the discharge. However, for the inception of the discharge we found that this overshoot is necessary. We try different values for the overshoot (in amplitude and duration) to obtain the best agreement between the experimental and the calculated current when the stationary state is reached. The voltage V_G applied to the gap is an input function of time as shown in Fig. 9. The ionic and electronic densities are defined by a mean value of the electric field

$$n_e(x) = n_e(0)\exp(\bar{\alpha}x) , \tag{31}$$

with $n_e(0) = 1.212 \times 10^{-14}$ C cm^{-3}, $\bar{\alpha} = 2.902$ cm^{-1}, $n_+(x) \approx \varepsilon_0(\partial E/\partial x) \approx 2.473 \times 10^{-11}$ cm^{-3}.

7. *Numerical procedure*

The applied mathematical model is composed of the ensemble of a set of partial differential equations. We have used as a numerical technique the method of flux-corrected transport described by Boris and Book [22,23]. Although this procedure has the best performance in treating such types of problems, it can present some difficulties especially concerning the anode and cathode boundary conditions when used in the analysis of gas discharges, as treated in detail by Morrow [24]. However, the stability of the method is remarkable, as compared to the method of characteristics, and permits in particular the treatment of delicate problems such as the inversion of electric field which appears in the negative glow.

III. RESULTS

A. Analysis of results in CO_2

A comparison is made between the results of the simulation with the two distribution functions, that of Lucas and that of Maxwell, obtained with the same experimental conditions and with the same numerical procedure. We will analyze the differences between the main parameters of the discharge.

In a qualitative approach, a similar evolution of the fundamental values of the discharge is obtained. This means that a Maxwellian distribution function is a good approximation if the temperature is correctly estimated (by means of the energy equation, for example).

In a quantitative approach, the results are different. The spatiotemporal evolution of the discharge shows great local differences.

Figure 1 shows a comparison between the spatiotemporal evolution of the electron density obtained with the two formalisms. The use of a Maxwellian distribution function (dashed line) gives rise to higher gradients that enhance ionization in the transition zone between the cathodic fall and the negative glow. All nonhydrodynamic phenomena become more pronounced. The choice of a Maxwellian distribution leads to a forced over-evaluation of nonequilibrium effects. This artificial overestimation of these nonequilibrium effects gives rise to an extremely unsteady discharge with very quick temporal evolution and diverging without reaching steady state after 72.5 ns. The use of the Lucas formalism gives rise to weaker gradients. The steady state of the discharge is reached after 250 ns. The calculations have been continued to 350 ns with a time step $\Delta t = 2.5 \times 10^{-2}$ ns; the calculation is very stable. The curves obtained during this calculation superimpose together very well.

The stationary state reached by the discharge is characterized by Townsend's criterion, and the maintenance condition for stationary state is

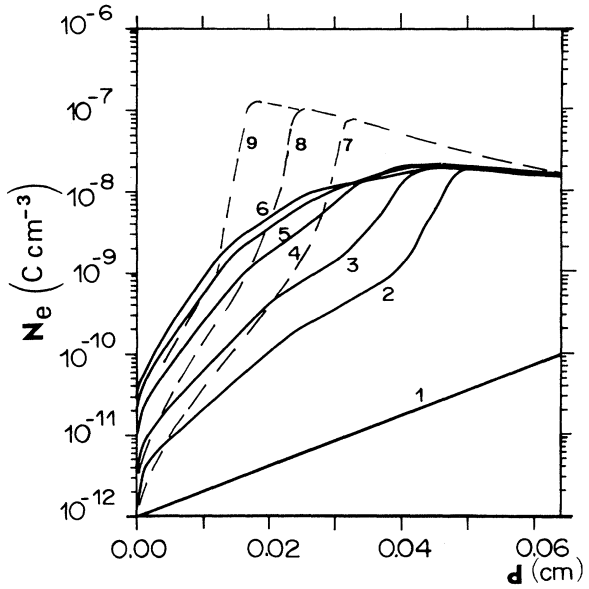

FIG. 1. Spatiotemporal evolution of electron density (in CO_2), comparison between the simulation with the Lucas distribution function (FL) and with the Maxwell distribution function (FM). (Curve 1) Initial conditions: identical for the two formalisms. The formalisms using the Lucas distribution function (solid lines); (2) $t = 50$ ns, (3) $t = 100$ ns, (4) $t = 150$ ns, (5) $t = 200$ ns, (6) $t > 250$ ns (stationary state). The formalism using the Maxwell distribution function (dashed lines); (7) $t = 25$ ns, (8) $t = 50$ ns, (9) $t = 72.5$ ns.

$$\gamma+\int_0^d \alpha_i(x)\exp\left\{\int_0^x\left[\alpha_i(x')-\alpha_a(x')\right]dx'\right\}dx+\gamma_{\mathrm{ph}}\int_0^d \alpha_{\mathrm{exc}}(x)\exp\left\{\int_0^x\left[\alpha_i(x')-\alpha_a(x')\right]dx'\right\}dx=1\ , \tag{32}$$

with α_i the ionization coefficient, α_a the attachment coefficient, and α_{exc} the excitation coefficient. These coefficients are deduced from the corresponding frequencies divided by the electron velocity. This formula applied to our simulation gives 0.94 for CO_2 for conditions of Fig. 2. Figure 2 shows the spatial evolution of the parameters in the discharge having reached the stationary state with a self-consistent model using a Lucas distribution function. Different zones are easy to recognize: the cathodic fall (CF) with an electric field which decreases quasilinearly and the negative glow (NG) with a weak electric field. Imbalance between the electron energy and the electric field is clear, particularly in the CF-NG transition and in the NG where the electron temperature is clearly higher than that deduced directly from the local electric field.

From the state of the discharge defined in Fig. 2, we tried to compare the Lucas distribution to the Maxwell distribution. Both of these distribution functions are calculated involving the temperature deduced from our model (temperature values given in Fig. 2). This comparison allows an estimation of the role of electron density gradients and of the electric field on the electron-energy distribution.

Figure 3 shows the comparison between the Maxwell and Lucas distribution functions when the discharge reaches a stationary state, the distribution functions showing the same differences in a transient state. This comparison on the microscopic state has been made in referenced points (1)–(4) in Fig. 2. In these points, the Maxwellian distribution function is calculated with the value of the temperature given in Fig. 2.

There is a strong spatial dependency of the distribution function (whatever the distribution function, Lucas or Maxwell) versus the distance from the cathode, linked to the local electric field and density gradient. The evolution of the distribution function shows that three zones can be distinguished.

(1) A first zone near the cathode where electrons are emitted from the cathode with a mean energy of 10 eV are greatly accelerated by a strong electric field. In spite of a strong gradient of density in this zone, this gradient plays a negligible role in the distribution function. Since the high value of the electric field will tend to eliminate the effect of $(1/n_e)\partial n_e/\partial x$ as explained in Eq. (1), the electrons emitted by the cathode are mainly influenced by the electric field. This zone can be defined as an adjustment zone for secondary electrons emitted by the cathode. In this zone of strong acceleration, the electrons are mainly fast ones. On this short distance, the elastic and inelastic collisions are not able to settle a process of collisional losses that could balance the gains induced by the electric field.

(2) A second zone in the negative glow, on the anode side, is a zone of weak electric field with weak electron mean energies. The gradient of electron density is nearly equal to zero and the density of electron current is spatially constant. The two distribution functions (Maxwell and Lucas) are very similar with a maximum of electrons in the bulk of the distribution function. This shows that the electron energy gained in the cathode fall is lost by the elastic collisional processes as will be detailed in the analysis of N_2 discharge.

(3) An intermediate zone which is a strong gradient zone. All the parameters of the discharge (electric field, densities, energy) vary greatly. In this zone, both the electric and the electron energy are very high. The energetic balance of electrons depends on two mechanisms: The first one is the inelastic collisions, and it is clear that ionization plays a great role in inducing a very strong electron growth. The second one involves strongly anisotropic elastic collisions in which the electron density gradient occurs as suggested by Saelee and Lucas [25] and Wedding, Blevin, and Fletcher [12]. These effects are clearly demonstrated by the Lucas distribution function which shows a deficit of high-energy electrons and an ex-

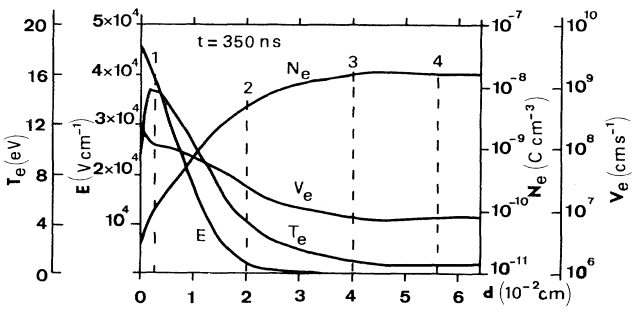

FIG. 2. Spatial distribution of the main parameters of the stationary discharge ($t=350$ ns).

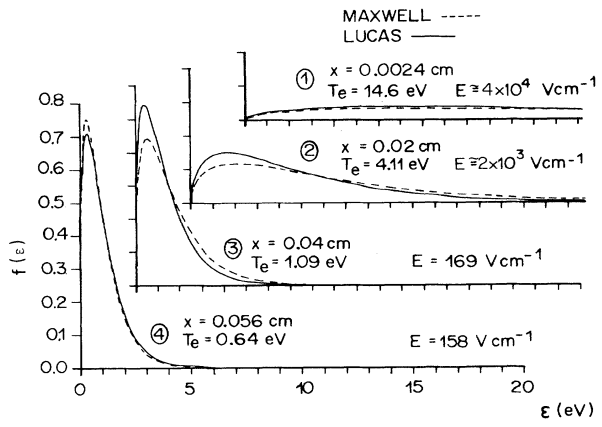

FIG. 3. Comparison between the distribution function of the Lucas (solid line) and the Maxwell distribution functions (dashed line) at points (1), (2), (3), and (4) of Fig. 2.

cess of low-energy electrons whereas the Maxwell distribution function is inefficient in presenting the whole elastic and inelastic collisions.

Figure 4 shows the spatiotemporal evolution of the electron velocity obtained by modeling the discharge with the Lucas distribution function. These curves are compared with the corresponding ones obtained using the Maxwellian distribution function (dashed line).

A high velocity is obtained near the cathode where the field effect is more important. At the transition zone between the cathode fall and the negative glow, the velocity is strongly reduced (by 2 orders of magnitude). This strong reduction in the velocity acts consequently on the discharge: The large number of electrons arriving from the cathode fall (secondary emission being followed by amplification) gather at the beginning of the negative glow as the velocity is too low to drain them and thus an excess of negative charge is observed. This point constitutes the fundamental difference in the discharge resulting from the use of the two models of distribution functions.

With the Lucas distribution function, which seems more accurate, the electron density gradient induces an enhancement of the velocity in the negative glow. The electrons arriving from the cathode fall are swept away toward the anode with a correct velocity. There is no charge gathering. The discharge is stabilized and becomes stationary when the electron velocity in the negative glow is high enough to sweep away the electrons, avoiding a negative charge storage. With the Maxwellian distribution function, there is a strong decrease of the velocity at the transition between the cathode fall and the negative glow. There is a strong charge increase, leading to a numerical divergence and the quality of being physically unable to give a stationary state.

The electron density variation (Fig. 1) shows clearly that the stationary state is represented by the curves. In these curves, there is a constant increase of the density induced by multiplication in the high field zone and a zone of constant density which represents the balance between the two-electron flux. With the Maxwellian function, an electron maximum appears at the transition between the cathode fall and the negative glow, moves with this transition, and is amplifying with time, showing a charge increase due to the imbalance between the electron fluxes arriving from cathode fall and those penetrating the negative glow.

Figure 5 shows the evolution of the electronic temperature. Two zones appear as in the electron velocity, a zone of high electron temperature near the cathode and a zone of low temperature near the negative glow. As for the other parameters, the transition between the two zones is smoother with the Lucas distribution function. The temperature in the negative glow is not equal to zero.

Figure 6 shows the evolution of the electric field. The classic variation is obtained with a quasilinear decrease in the cathode fall, and a very weak electric field in the negative glow. Two observations can be made. The first one concerns the spatial variation of the electric field compared to that of the electron temperature. In the transition between the cathode fall and the negative glow, the temperature decreases more weakly than the electron field. A non-null energy exists in the beginning of the negative glow, showing an imbalance effect, partially slitting the electrons from the electric field. The local electron energy depends not only on the local values of the

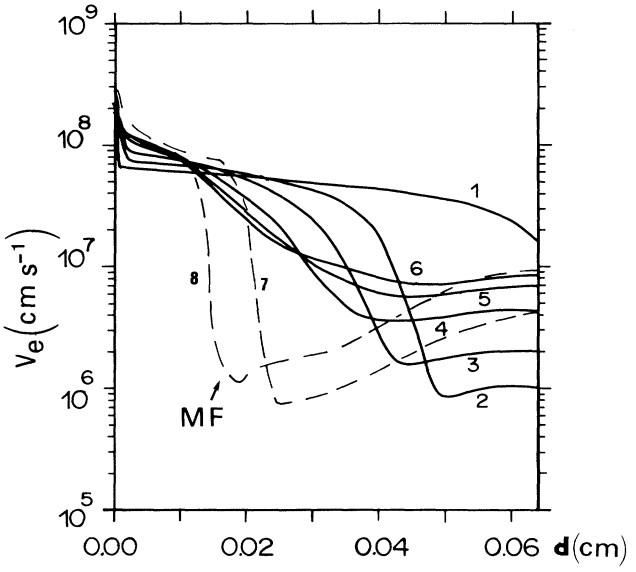

FIG. 4. Spatiotemporal evolution of electron velocity. (Curve 1) Initial conditions. The formalism using the Lucas distribution function (solid lines); (2) $t=50$ ns, (3) $t=100$ ns, (4) $t=150$ ns, (5) $t=200$ ns, (6) $t>250$ ns (stationary state). The formalism using the Maxwell distribution function (MF) (dashed lines); (7) $t=50$ ns, (8) $t=72.5$ ns.

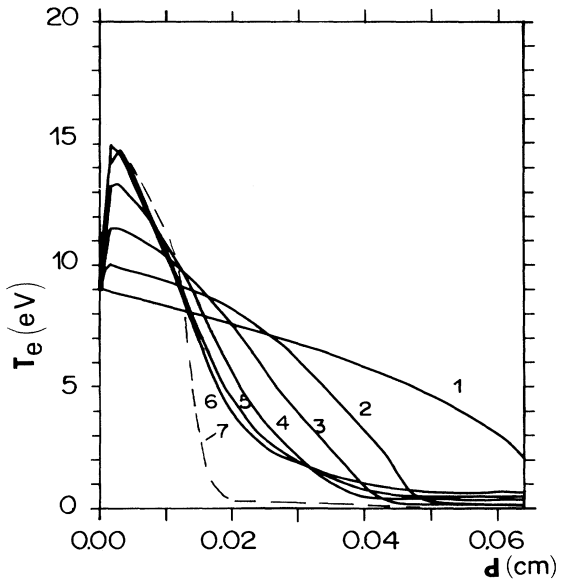

FIG. 5. Spatiotemporal evolution of electron temperature. (Curve 1) Initial conditions. The formalism using the Lucas distribution function (solid lines); (2) $t=50$ ns, (3) $t=100$ ns, (4) $t=150$ ns, (5) $t=200$ ns, (6) $t>250$ ns (stationary state). The formalism using the Maxwell distribution function (dashed line); (7) $t=72.5$ ns.

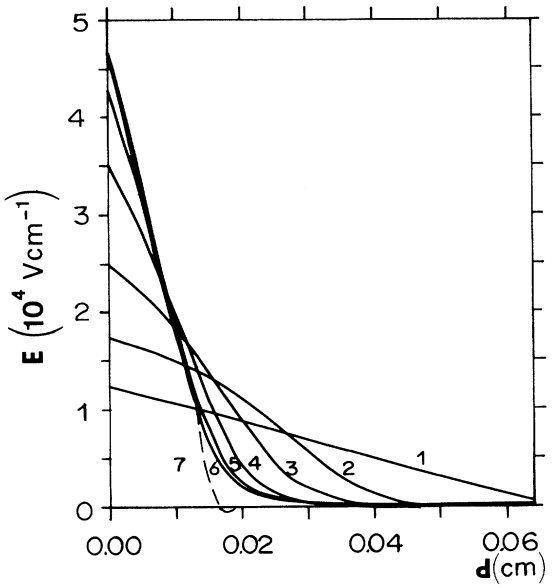

FIG. 6. Spatiotemporal evolution of electric field. (Curve 1) Initial conditions. The formalism using the Lucas distribution function (solid lines); (2) $t=50$ ns, (3) $t=100$ ns, (4) $t=150$ ns, (5) $t=200$ ns, (6) $6>250$ ns (stationary state). The formalism using the Maxwell distribution function (dashed line); (7) $t=72.5$ ns.

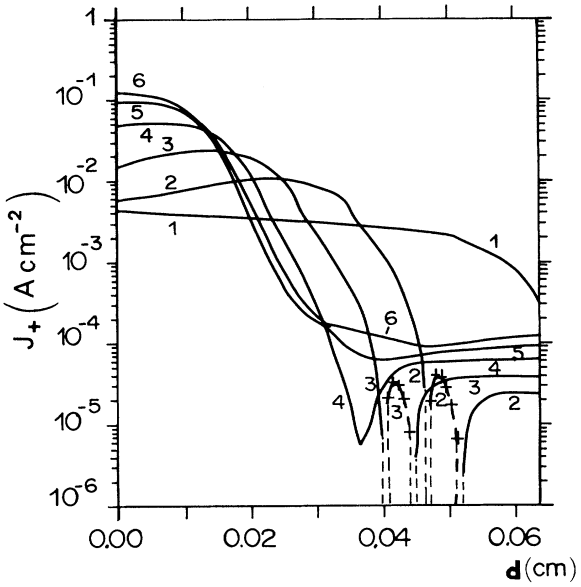

FIG. 7. Spatiotemporal evolution of current density of positive ions. The formalism using the Lucas distribution function (solid lines). (Curve I) Initial conditions, (2) $t=50$ ns, (3) $t=100$ ns, (4) $t=150$ ns, (5) $t=200$ ns, (6) $t>250$ ns (stationary state). The dashed lines in curves 2 and 3 point out a change in ion current direction (and thus an electric field local inversion too weak to be observed in Fig. 6).

electric field but also on the local values of the gradients of densities $(1/n_e)\partial n_e/\partial x$ and of energy $(\partial n_e kT_e/\partial x)$;$(\partial n_e kT_e u_e/\partial x)$. This has already been observed in [7] and [9].

The use of the Lucas distribution function which, including in its formulation the gradient effects, enhances the differences between the field and the temperature evolutions.

The second observation concerns the field inversion. This inversion is weak with a maximum value of about 60 V/cm lasting for 40–110 ns. After this, the electric field again becomes positive. It is interesting to notice that field inversions have been noted in experimental works (in gases other than those studied here) by Warner, Conner, and Woods [26] and by Den Hartog, Doughty, and Lawler [27]. The theoretical results obtained in this work confirm these observations.

The scale of Fig. 5 does not permit the perception of the inversion which is easier to analyze in Fig. 7.

The velocity of the positive ions, which is directly proportional to the electric field $(v_+=\mu_+E)$, is reversed at $t=50$ ns and $t=100$ ns. Of course, as the electron velocity is deduced from the momentum equation there is no inversion on it.

This field inversion, which is transitory with the Lucas distribution function, remains permanently with the Maxwellian distribution function and enhances the charge storage effect, reducing the velocity in the transition zone between the cathode fall and the negative glow. It is necessary to remark that the decrease of the electric field is weaker with the Lucas distribution function and allows a better draining of the positive ions toward the cathode and thus promotes the stationary conditions.

The efficiency of the good draining for electrons and positive ions in the inception and the maintenance of the stationary state appears clear in Fig. 8 where the electron current density is noticeably steady in the negative glow and the positive current is steady in the cathode fall.

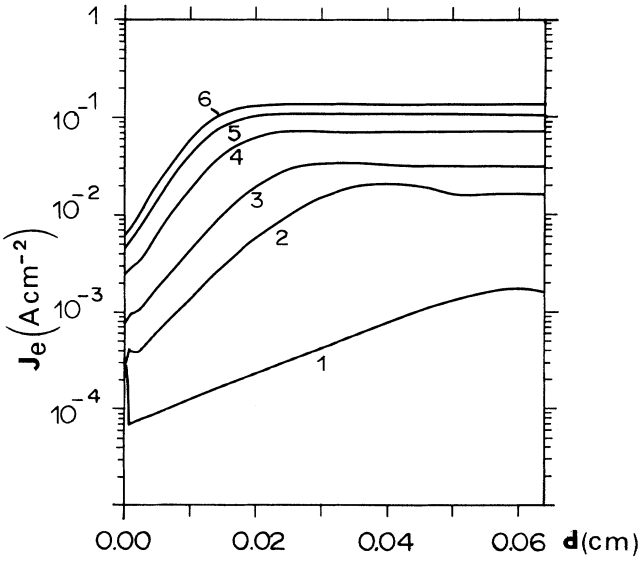

FIG. 8. Spatiotemporal evolution of electron current density. The formalism using the Lucas distribution function (solid lines). (Curve 1) Initial conditions, (2) $t=50$ ns, (3) $t=100$ ns, (4) $t=150$ ns, (5) $t=200$ ns, (6) $t>250$ ns (stationary state).

B. Analysis of the results in N_2

After testing the presented model composed of the macroscopic transport equation and the Lucas microscopic distribution function, in simulating the discharge in CO_2, we test the validity of the model in the case of nitrogen. Actually, nitrogen gas has well-known collision cross sections as well as macroscopic coefficients, and simulating the discharge in nitrogen by a theoretical model can be a good test for the validity of such a model. We simulate the experiment of Bastien, Wu, and Marode [10]. In this experiment, the authors have studied the luminous emission of nitrogen discharge at low pressure. The experimental conditions are pressure $P=1$ Torr, the gap is 2 cm, the electrode diameter is 45 mm. They measured the electric current, the voltage, and the optical luminous emission in the gap. Since the pressure is low, the cathodic region (cathode fall and negative glow) is extended all over the gap. The analysis of light emission concerns the packet centered at $\lambda=3914$ Å of the negative system $B\,^2\Sigma_u^+(v=0)\rightarrow X\,^2\Sigma_g(v'=0)$ and that $\lambda=3577$ Å of the second positive system $C\,^3\Pi_u(v=0)\rightarrow B\,^3\Pi_g(v'=1)$. Our simulation of the experiment is based on the described model (hydrodynamic equations plus the Lucas distribution function). The data concerning the gas pressure, gap distance, and the applied voltage are given in the simulation. The quantities subjected to correlation are the total electric current and the spatial luminous emission which is computed with Eq. (5). The comparison of these two values induces correlations strong enough to state that the other values (charge carrier densities, electronic velocity, and electronic temperature) are accurate if these two values fit with the experimental ones.

The stabilization voltage is 540 V. The overshoot conditions as estimated in the simulation will give a theoretically stationary discharge current of $I_{th}=25$ mA as shown in Fig. 9. It is worthwhile to state that the value of the deviation of the theoretically stationary current with respect to that measured experimentally varies only weakly around an average value which is the experimental one. The time elapsed until the stationary discharge is

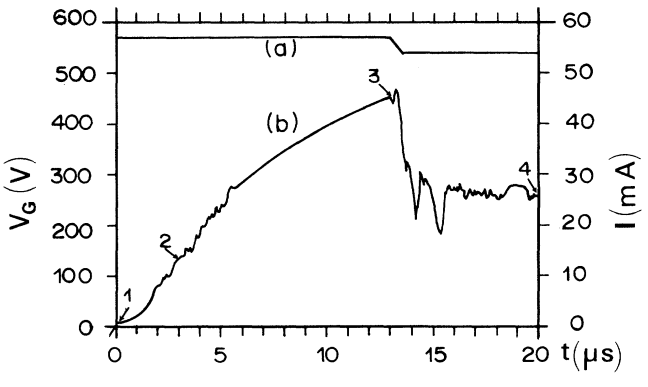

FIG. 9. Temporal voltage (a) and current (b) evolutions in N_2. The voltage is experimental data. The current is calculated by the model with the Lucas distribution function.

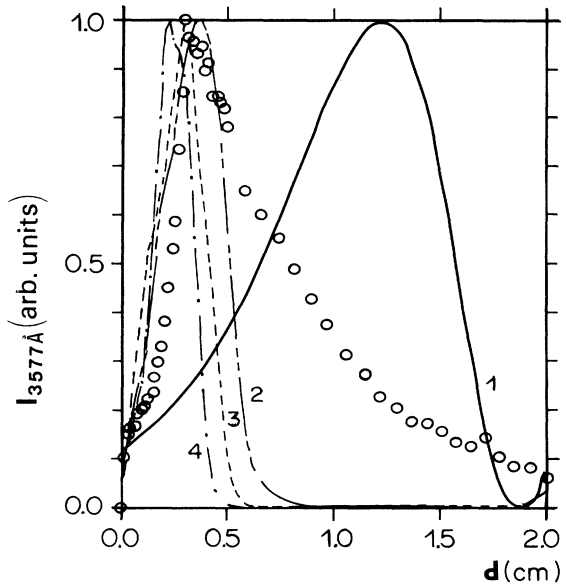

FIG. 10. Spatiotemporal evolution of light emission ($\lambda=3577$ Å). The open circles denote experimental values from [10]; (Curve 1), initial conditions of the simulation, (2) $t=3$ μs, (3) $t=13$ μs, (4) $t=20$ μs (stationary state).

established in the simulation model depends on the initial conditions. On the contrary, the simulated spatial light emission does not depend on the theoretical initial conditions and seems to depend only on the discharge data (i.e., pressure, gap length, voltage). Figure 10 shows how the luminous emission of the first negative system evolves towards being stationary while curves 1–4 correspond to points 1–4 in Fig. 9. The correspondence between the position of the simulation maximum luminosity and the experimental one can be observed clearly. The difference in the spatial extension between the theoretical and experimental luminosity curves may be explained from a theoretical point of view. The choice of the Lucas distribution function yields a good average microscopic behavior of the nonequilibrium electron isotropic (or bulk) distribution but it does not consider the different specific excitation mechanisms and the anisotropy of the distribution. Since we have obtained good agreement with experiment concerning both the electric current and the spatial luminous emission it will be interesting to consider other quantities in the stationary discharge. Figure 11 gives

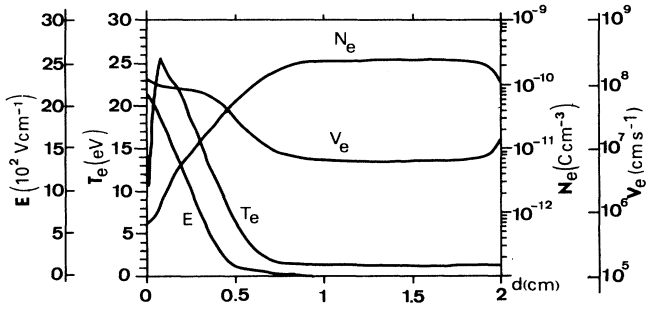

FIG. 11. Spatial evolution of the main parameters in the discharge at stationary state (point 4 of Fig. 9) in N_2.

the spatial distribution of the electric field, electron temperature, density, and drift velocity at the stationary state, the maintenance condition (32) gives 0.92 for this situation. Here we can locate the same characteristic zones as in the CO_2.

IV. CONCLUSION

The formalism proposed in this paper allows one to simulate successfully the inception of the cathode zone up to the steady state in CO_2 and N_2 taking into account nonequilibrium between the electrons and the field. This shows that it is possible to study discharges in nonhydrodynamic situations by means of a formalism deduced from the successive moments of the Boltzmann equation.

The use of the collisional operators sensitive to the shape of the distribution function allows one to simplify the formalism but preserves all its efficiency. Those of the operators which mainly depend on the bulk of the distribution function are stated macroscopically, that is to say, simply. Those which depend on the tail of the distribution function (ionization, excitation) are microscopically stated by means of a distribution function taking into account the gradient effects in the discharge.

*Present address: Université Paul Sabatier, 31062 Toulouse Cedex, France.

[1] J. P. Boeuf and E. Marode, J. Phys. D **15**, 2169 (1982).
[2] T. J. Moratz, L. C. Pitchford, and J. N. Bardsley, J. Appl. Phys. **61**, 2146 (1987).
[3] T. J. Sommerer, J. E. Lawler, and W. N. G. Hitchon, J. Appl. Phys. **64**, 1775 (1988).
[4] D. A. Doughty, E. A. Den Hartog, and J. E. Lawler, Phys. Rev. Lett. **58**, 2668 (1987).
[5] A. V. Phelps, B. M. Jelenkovic, and L. C. Pitchford, Phys. Rev. A **36**, 5327 (1987).
[6] T. J. Sommerer, W. N. G. Hitchon, and J. E. Lawler, Phys. Rev. A **39**, 6356 (1989).
[7] P. Bayle, J. Vacquie, and M. Bayle, Phys. Rev. A **34**, 360 (1986); **34**, 372 (1986).
[8] I. Abbas and P. Bayle, J. Phys. D **14**, 649 (1981); **14**, 661 (1981).
[9] P. Bayle and B. Cornebois, Phys. Rev. A **31**, 1046 (1985).
[10] F. Bastien, H. Wu Jiang, and E. Marode, in IX International Conference on Gas Discharges and Their Applications, Venice, 1988, p. 395.
[11] J. E. Lawler, Phys. Rev. A **32**, 2977 (1985).
[12] A. B. Wedding, H. A. Blevin, and J. Flechter, J. Phys. D **18**, 2361 (1985).
[13] A. B. Wedding and L. J. Kelly, Aust. J. Phys. **42**, 101 (1989).
[14] W. R. L. Thomas, J. Phys. B **2**, 551 (1969).
[15] K. Kumar, H. R. Skullerud, and R. R. Robson, Aust. J. Phys. **33**, 343 (1980).
[16] J. Lucas, Int. J. Electron. **22**, 529 (1967); **29**, 465 (1970).
[17] H. N. Kucukarpaci and J. Lucas, J. Phys. D **12**, 2123 (1979).
[18] G. Hartmann, Thèse, Université Paris VI-Orsay, Report No. 1783, 1977 (unpublished).
[19] J. D. Cobine, *Gaseous Conductors* (Dover, New York, 1958).
[20] A. I. Ivanchenko and A. A. Shepevenko, Teplofiz. Vys. Temp. **20**, 636 (1982).
[21] G. Francis, *Ionization Phenomena in Gases* (Butterworths, London, 1960).
[22] J. P. Boris and D. L. Book, in *Methods in Computational Physics,* edited by John Killeen (Academic, New York, 1976), pp. 85–130.
[23] D. L. Book, *Finite Difference Techniques for Vectorized Fluid Dynamics Calculations* (Springer-Verlag, New York, 1981).
[24] R. Morrow, in XVIII International Conference on Phenomena in Ionized Gases, Venice, 1987.
[25] H. T. Saelee and J. Lucas, J. Phys. D **10**, 343 (1977).
[26] H. E. Warner, W. T. Conner, and R. C. Woods, J. Chem. Phys. **81**, 5413 (1984).
[27] E. A. Den Hartog, D. A. Doughty, and J. E. Lawler, Phys. Rev. A **38**, 2471 (1988).